Energy Conversion and Management 50 (2009) 2879–2884

Contents lists available at ScienceDirect

Energy Conversion and Management

journal homepage: www.elsevier.com/locate/enconman

Soft switching bidirectional DC–DC converter for ultracapacitor–batteries interface

Ehsan Adib *, Hosein Farzanehfard

Department of Electrical and Computer Engineering, Isfahan University of Technology, Iran

ARTICLE INFO

Article history:
Received 21 October 2008
Received in revised form 28 June 2009
Accepted 20 July 2009
Available online 22 August 2009

Keywords:
Battery
DC–DC power converters
Ultracapacitor
Soft switching

ABSTRACT

In this paper a new soft switching bidirectional DC–DC converter is introduced which can be applied as the interface circuit between ultracapacitors and batteries or fuel cells. All semiconductor devices in the proposed converter are soft switched while the control circuit remains PWM. Due to achieved soft switching condition, the energy conversion through the proposed converter is highly efficient. The proposed converter is analyzed and a prototype converter is implemented. The presented experimental results confirm the theoretical analysis.

1. Introduction

The energy storage systems are designed to provide peak power demands. If only batteries or fuel cells are used in an energy storage system, their capacity should be over designed to provide the peak power stresses. By using ultracapacitor besides batteries or fuel cells, the peak power demands can be provided using ultracapacitors and therefore, the energy storage devices are designed to provide only the average power required. Therefore, by combining the ultracapacitors and batteries or fuel cells, the volume and cost of the energy storage elements can be decreased. The ultracapacitors are charged usually through the energy storage elements such as batteries and fuel cells when the power demand is low. At peak power, the stored energy in the ultracapacitor will support the energy storage devices to provide the required power.

Ultracapacitors are a new generation of capacitors that have extremely high capacity but the voltage they can tolerate is small. Although ultracapacitors have higher power density than batteries, their energy density is much lower. In order to combine the ultracapacitors and energy storage elements such as batteries and fuel cells, a bidirectional interface circuit is required. The interface circuit charges the ultracapacitor at low power demands and discharges the ultracapacitor at peak power demands. DC–DC converters are vastly applied in industry as interface circuits [1–3]. Usually buck and boost converter is used as the interface circuit of batteries and ultracapacitors [4,5]. The converter charges the ultracapacitors in buck mode since their voltage is low and discharges the ultracapacitors in boost mode to adapt the low capacitors voltage to higher voltage of batteries. In order to reduce the size and weight of this converter, high switching frequency is indispensable. However, at high frequencies the converter efficiency is reduced due to switching losses and thus, the energy is wasted while charging and discharging the ultracapacitors. Switching losses are produced at switching instances where both the voltage across the switch and the current through the switch have considerable value. By limiting the current or voltage at switching instant, switching losses are eliminated which is called soft switching. Therefore, soft switching techniques can be applied to the interface circuit to eliminate the switching losses and improve the converter efficiency while decreasing the Electro Magnetic Interferences (EMI) [6–10]. The introduced soft switching interface circuit in [9] is a bidirectional isolated converter. In many applications isolation is not necessary and only the total efficiency decreases due to isolation while no desirable benefit is achieved. Also, isolation increases the converter volume and weight. A ZVT PWM buck and boost converter is introduced in [10], however, in this converter the control circuit is complicated and the auxiliary circuit is used twice in every switching cycle. In soft switching converters the switching losses are recovered using additional circuit elements. In other words, in soft switching converters especially in ZVT and ZCT type converters, although the conduction losses of the auxiliary circuit are added, but the switching losses are recovered. Since the conduction losses of the auxiliary circuit are much less than the switching losses, the efficiency increases using these techniques. In the converter of [10], the auxiliary circuit is applied two times in a switching cycle. This means that in the

* Corresponding author. Address: Electrical and Computer Engineering Department, Isfahan University of Technology, Isfahan 84156, Iran. Tel.: +98 9133658147; fax: +98 3113912451.
E-mail addresses: adib.ehsan@gmail.com (E. Adib), hosein@cc.iut.ac.ir (H. Farzanehfard).

0196-8904/$ - see front matter © 2009 Elsevier Ltd. All rights reserved.
doi:10.1016/j.enconman.2009.07.001

converter of [10], the additional conduction losses are almost twice the proposed converter for recovering the same amount of switching losses. Therefore, the proposed converter has better efficiency than converter of [10] while the required control circuit for the auxiliary circuit is much simpler.

In this paper a soft switching PWM buck and boost converter is introduced which uses an auxiliary circuit only once at switching instant in each switching cycle. Therefore, the control circuit is simple and also the auxiliary circuit losses are low. The proposed converter is introduced and analyzed in Section 2. Design considerations are discussed in Section 3. In Section 4, the experimental results are presented which confirm the validity of theoretical analysis.

2. Circuit description

The proposed interface circuit is shown in Fig. 1. The main bidirectional buck and boost converter is composed of two bidirectional switches S_1 and S_2 and filter inductor L. The auxiliary circuit is composed of a bidirectional switch S_{a1}, a unidirectional switch S_{a2}, two small resonant inductors L_r and L_S, and a small resonant capacitor C_r. The auxiliary circuit provides the soft switching condition for S_1 and S_2 while its semiconductor devices are also soft switched. In order to simplify the theoretical analysis, it is assumed that all semiconductor devices are ideal. Also, inductor L is large enough to assume its current is constant in a switching cycle. The converter operation is analyzed in both buck mode and boost mode.

2.1. Buck mode operation

The converter operation in buck mode is composed of six different operating intervals in a switching cycle. The converter theoretical waveforms are shown in Fig. 2 and equivalent circuit for each operating interval is shown in Fig. 3. Before the first interval it is assumed that C_r voltage is zero, D_2 is conducting the current through L (I_0), and all other semiconductor devices are off.

Interval 1 [$t_0 - t_1$]: This interval starts by turning S_1 on and since D_2 is conducting, the battery voltage (V_{bat}) is place across L_r and its current increases linearly. Therefore, this switch turns on under zero current (ZC) condition. L_r current equation during this interval is:

$$I_{Lr} = \frac{V_{bat}}{L_r}(t - t_0) \tag{1}$$

At the end of this interval, L_r current reaches I_0 and D_2 turns off under ZC condition.

Interval 2 [$t_1 - t_2$]: In this interval, energy is transferred from battery to ultracapacitor. Also, a resonance starts between L_r and C_r through D_{a1} and thus, C_r is charged to $2V_{bat}$. The current equation for L_r during this interval is:

$$I_{Lr} = I_0 + \frac{V_{bat}}{Z_0}\sin(\omega_0(t - t_1)) \tag{2}$$

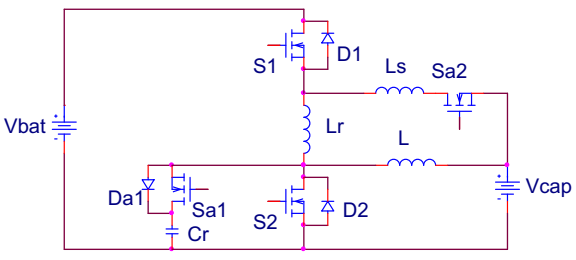

Fig. 1. Proposed soft switching interface circuit.

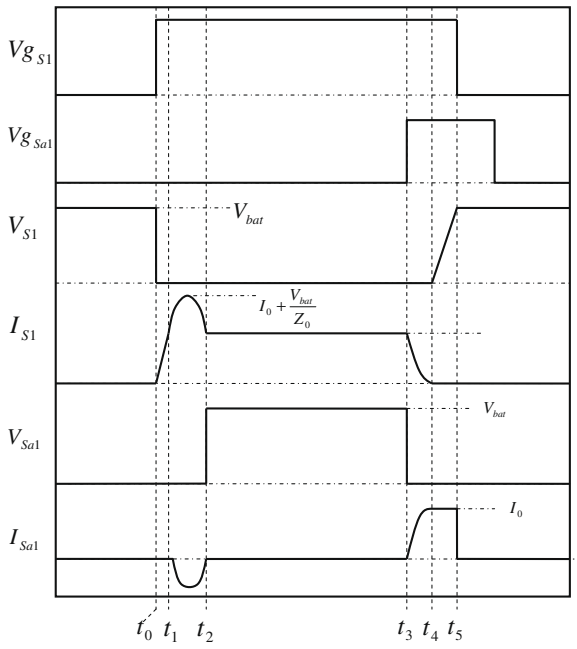

Fig. 2. Converter theoretical waveforms in buck mode.

where

$$Z_0 = \sqrt{\frac{L_r}{C_r}}, \quad \omega_0 = \frac{1}{\sqrt{L_r C_r}} \tag{3}$$

Interval 3 [$t_2 - t_3$]: In this interval, the energy is transferred from battery to ultracapacitor through S_1 and all other semiconductor devices are off.

Interval 4 [$t_3 - t_4$]: In this interval, S_{a1} is turned on and the difference between C_r voltage and the battery voltage is placed across L_r. Therefore, the current through L_r and S_1 is reduced to zero. At the end of this interval S_1 is turned off under ZC condition. L_r current during this interval is:

$$I_{Lr} = I_0 - \frac{V_{bat}}{Z_0}\sin(\omega_0(t - t_3)) \tag{4}$$

ZC condition for S_1 turn off is achieved if V_{bat}/Z_0 is greater or equal to I_0. Assuming V_{bat}/Z_0 is equal to I_0, C_r voltage is equal to V_{bat} at the end of this interval.

Interval 5 [$t_4 - t_5$]: During this interval, C_r is discharged by L current (I_0) until its voltage is reduced to zero and diode D_2 is forward biased.

Interval 6 [$t_5 - t_0 + T$]: Diode D_2 starts to conduct under zero voltage (ZV) condition and L current runs through this diode.

2.2. Boost mode operation

The converter operation in boost mode has eight distinct operating intervals in a switching cycle. The converter theoretical waveforms are shown in Fig. 4 and equivalent circuit for each operating interval is shown in Fig. 5. Before the first interval it is assumed that D_1 is conducting the current through L_r and L (I_{in}) and all other semiconductor devices are off. Also, it is assumed that C_r voltage is $V_{bat} + Z_0 I_{in}$.

Interval 1 [$t_0 - t_1$]: This interval starts by turning S_{a1} and S_{a2} on. Since S_{a2} and D_1 are on, $V_{bat} - V_{cap}$ is placed across L_S and its current increases linearly to I_{in} and D_1 current reduces from I_{in} to zero accordingly. Therefore, S_{a2} is turned on under ZC condition and at the end of this interval D_1 turns off under ZC condition. L_S current equation during this interval is:

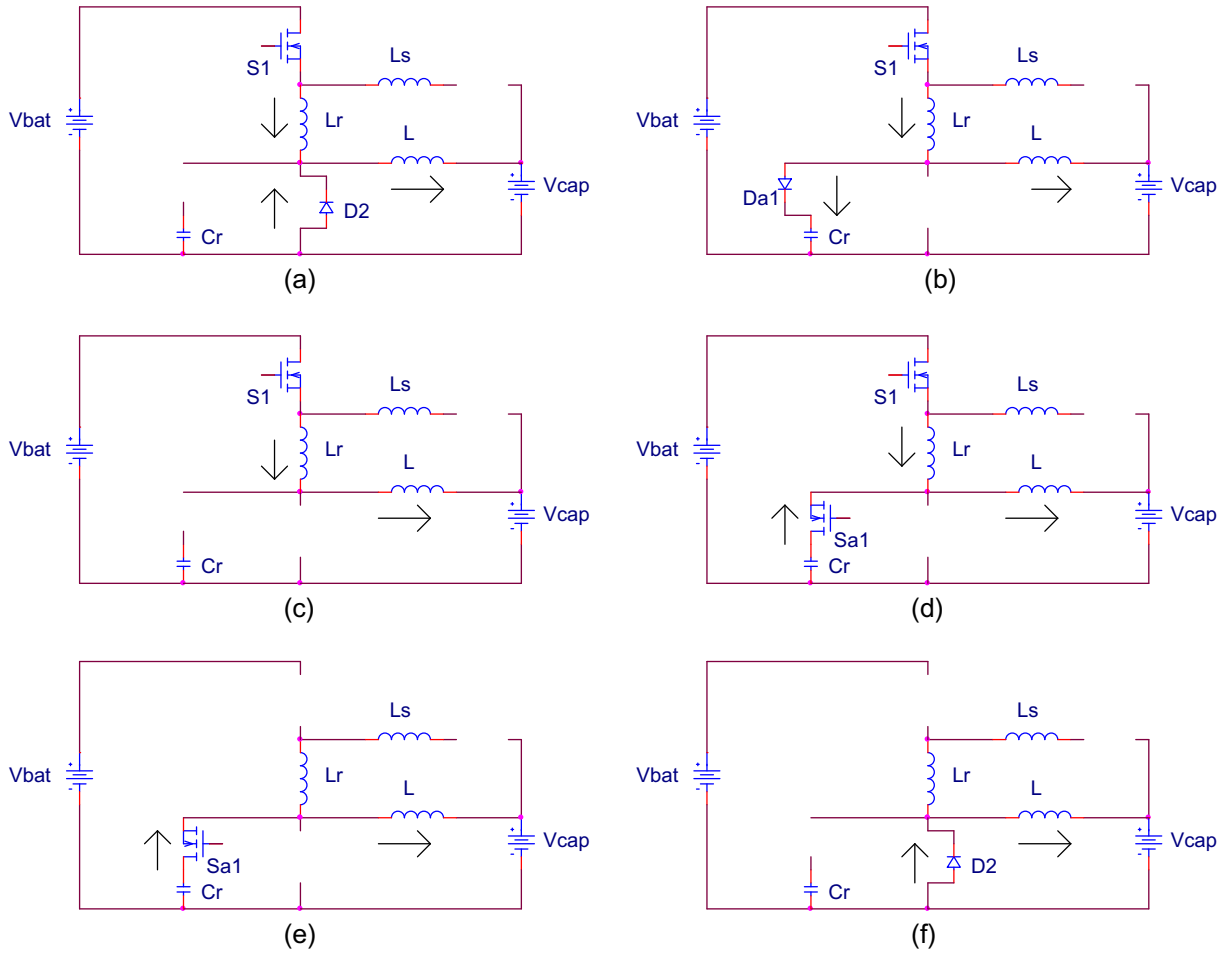

Fig. 3. Equivalent circuit for each operating interval of buck mode (a) $[t_0 - t_1]$ (b) $[t_1 - t_2]$ (c) $[t_2 - t_3]$ (d) $[t_3 - t_4]$ (e) $[t_4 - t_5]$ (f) $[t_5 - t_0 + T]$.

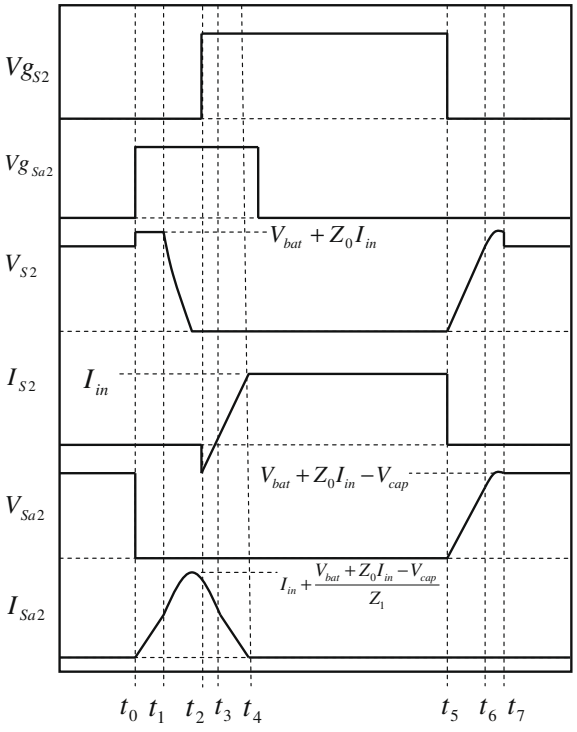

Fig. 4. Converter theoretical waveforms in boost mode.

$$I_{Ls} = \frac{(V_{\text{bat}} - V_{\text{cap}})}{L_S}(t - t_0) \tag{5}$$

Since the duration of this interval is small, it can be assumed that C_r voltage is almost constant during this interval.

Interval 2 $[t_1 - t_2]$: In this interval a resonance occurs between C_r, L_r and L_S and thus, C_r discharges in a resonance fashion. C_r voltage equation is:

$$V_{Cr} = (V_{\text{bat}} + Z_0 I_{\text{in}} - V_{\text{cap}})\cos(\omega_1(t - t_1)) + V_{\text{cap}} \tag{6}$$

where

$$\omega_1 = \frac{1}{\sqrt{(L_r + L_S)C_r}}, \quad Z_1 = \sqrt{\frac{L_r + L_S}{C_r}} \tag{7}$$

Interval 3 $[t_2 - t_3]$: When C_r voltage reaches zero, D_2 starts to conduct under zero voltage condition and V_{cap} is placed across series combination of L_S and L_r. Thus, the current in L_S and L_r decrease linearly to I_{in} where D_2 turns off under ZC condition. During this interval S_2 is turned on under ZV condition.

Interval 4 $[t_3 - t_4]$: V_{cap} is still across L_S and L_r and their current continues to decrease from I_{in} to zero and S_2 current increases from zero to I_{in} accordingly. L_r current equation during this interval is:

$$I_{Lr} = I_{\text{in}} - \frac{V_{\text{cap}}}{L_r + L_S}(t - t_3) \tag{8}$$

Interval 5 $[t_4 - t_5]$: S_2 is on and energy is being stored in L similar to a regular boost converter. Duration of this interval (converter duty cycle) is determined by control circuit according to control strategy.

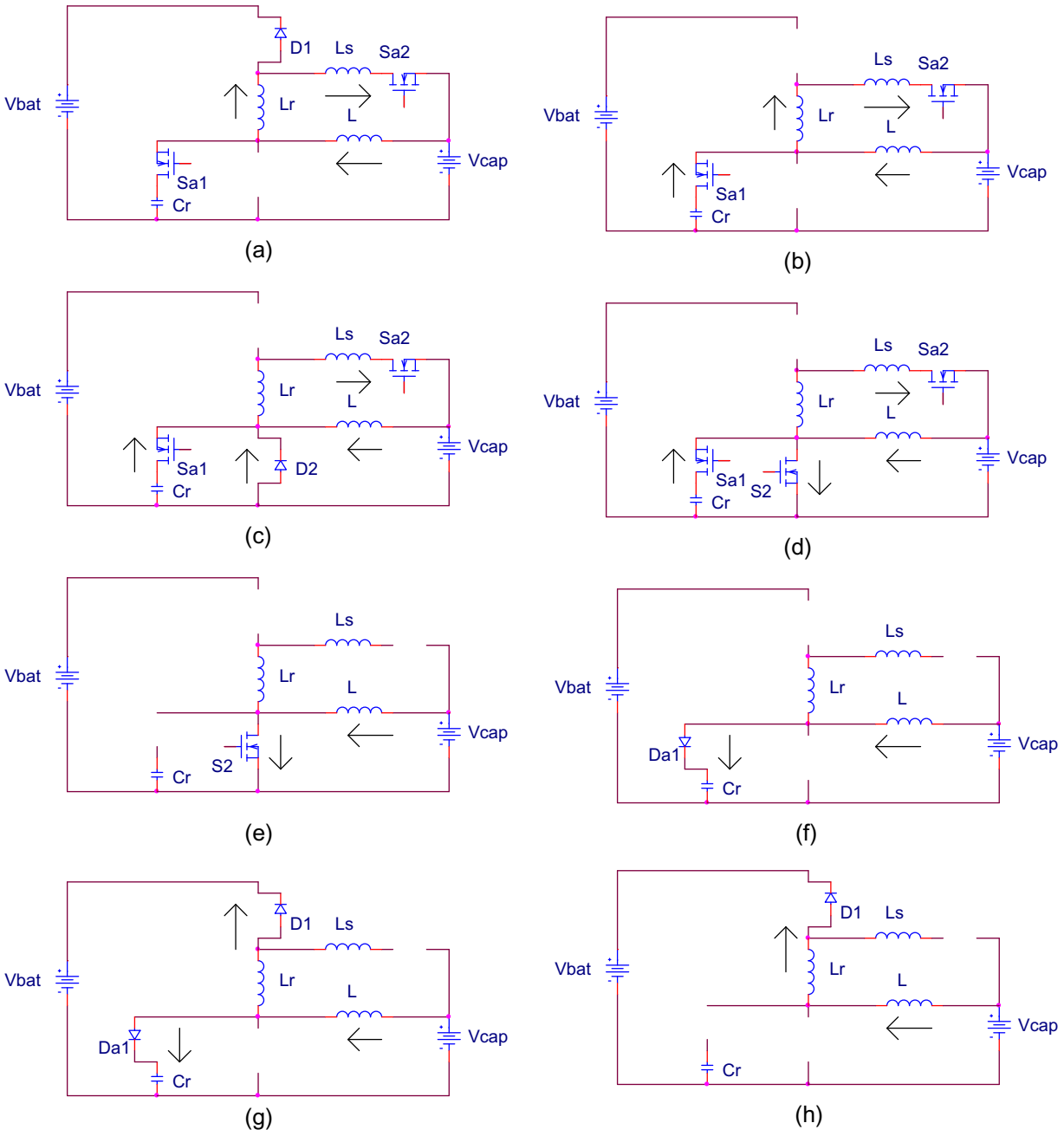

Fig. 5. Equivalent circuit of each operating interval of boost mode (a) $[t_0 - t_1]$ (b) $[t_1 - t_2]$ (c) $[t_2 - t_3]$ (d) $[t_3 - t_4]$ (e) $[t_4 - t_5]$ (f) $[t_5 - t_6]$ (g) $[t_6 - t_7]$ (h) $[t_7 - t_0 + T]$.

Interval 6 $[t_5 - t_6]$: S_2 is turned off and L current charges C_r through D_{a1}. Since C_r voltage changes linearly from zero to V_{bat}, thus, S_2 is turned off under ZV condition. C_r voltage during this interval is:

$$V_{Cr} = \frac{I_0}{C_r}(t - t_5) \tag{9}$$

Interval 7 $[t_6 - t_7]$: When C_r voltage reaches V_{bat}, a resonance occurs between C_r and L_r. Thus, L_r current increases from zero to I_{in} in a resonance fashion. Also, C_r voltage increase from V_{bat} to $V_{bat} + Z_0 I_{in}$. The equations of C_r voltage and L_r current during this interval are:

$$V_{Cr} = V_{bat} + Z_0 I_{in} \sin(\omega_0(t - t_6)) \tag{10}$$

$$I_{Lr} = I_{in}(1 - \cos(\omega_0(t - t_6)) \tag{11}$$

Interval 8 $[t_7 - t_0 + T]$: Diode D_1 turns on under ZV condition and energy is transferred from ultracapacitors to batteries.

3. Design considerations

Inductor L is designed like filter inductor of a regular PWM buck and boost converter. According to (4), in order to achieve ZC condition at S_1 turn off for the buck mode operation, the following condition should be achieved:

$$\frac{V_{bat}}{Z_0} \geqslant I_{0\max} \tag{12}$$

where I_{0max} is the maximum ultracapacitors charging current in buck mode. In practice 20% over design is necessary, therefore:

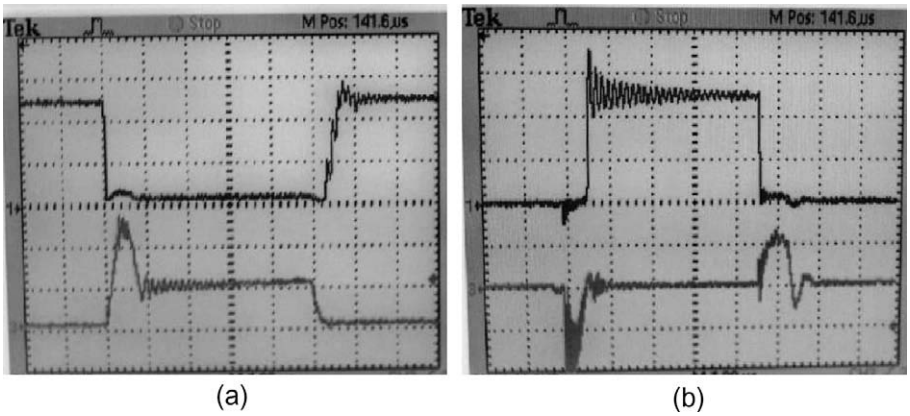

Fig. 6. Experimental results of buck mode, voltage (top waveform) and current (bottom waveform) of (a) main switch S_1 (b) auxiliary switch S_{a1} (vertical scale 20 V/div or 4 A/div, time scale 1us/div).

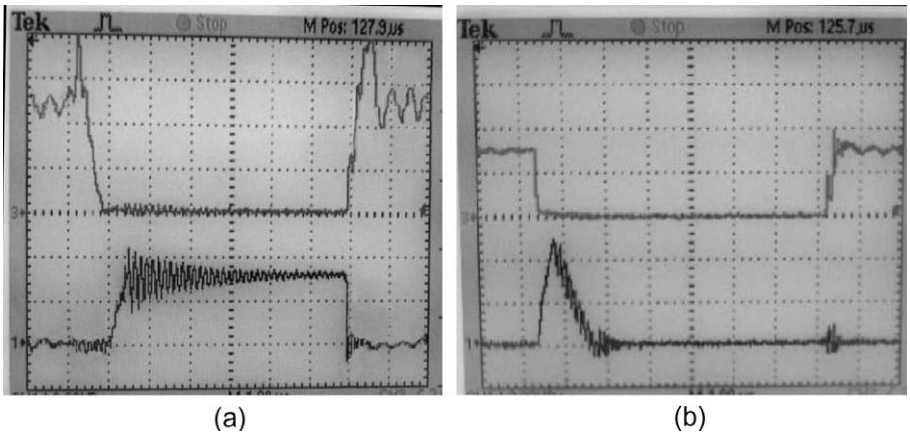

Fig. 7. Experimental results of boost mode, voltage (top waveform) and current (bottom waveform) of (a) main switch S_2 (b) auxiliary switch S_{a2} (vertical scale 20 V/div or 3 A/div, time scale 1 us/div).

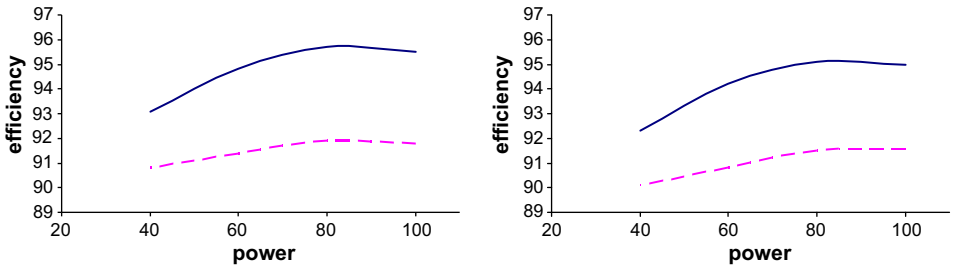

Fig. 8. Converter efficiency curve (continuous line) versus hard switching counterpart (broken line) (a) buck mode (b) boost mode.

$$Z_0 \leqslant \frac{V_{\text{bat}}}{1.2 I_{0\,\max}} \tag{13}$$

L_S provides ZC condition for S_{a2} turn on and L_r provide ZC condition for S_1 turn on. Thus, their values can be calculated like any turn on snubber. By calculating L_r, the value of C_r can be calculated using (13) and (3).

According to (6), in order to achieve ZV condition for S_2 turn on for the boost mode operation, the following condition should be achieved:

$$V_{\text{bat}} + Z_0 I_{\text{in,min}} \geqslant 2V_{\text{cap}} \tag{14}$$

where $I_{\text{in,min}}$ is minimum L current in boost mode. Since V_{bat} is usually more than twice the ultracapacitors voltage, the above condition is trivial.

4. Experimental results

In order to confirm the validity of theoretical analysis, a prototype converter is implemented. The batteries voltage is 48 V and the ultracapacitors voltage is 24 V. The converter operating power is 100 W and its switching frequency is 100 kHz. According to design procedure, a 200 uH inductor is used for L, a 1.5 uH inductor is used for L_r, a 1 uH inductor is used for L_S and 18 nF capacitor is used for C_r. IRF540 is used for all of the switches and for S_{a2}, a MUR460 is used as the series diode. The converter experimental results for buck mode are shown in Fig. 6 and boost mode experimental results are illustrated in Fig. 7. According to Fig. 6a, after the main switch S_1 is turned on, its voltage decreases to zero and then its current increases first linearly to I_0 and then in a resonance

fashion to its maximum value as it was predicted in the theoretical analysis. As it can be observed from the same figure, just before turning S_1 off, its current has decreased to zero. Therefore, zero current switching condition is achieved for S_1 that confirms the theoretical analysis and also the achieved soft switching condition for the auxiliary switch is apparent in Fig. 6b. As it can be observed in Fig. 7a, the S_2 voltage has decreased to zero and then this switch is turned on and the switch current increases to I_{in}. Furthermore, when S_2 is turned off, the voltage across it increases linearly to its final value as predicted in theoretical analysis. In addition, the presented experimental results in Fig. 7b, justify theoretical analysis of the proposed converter. The converter efficiency curve in buck mode and boost mode is compared with hard switching converters in Fig. 8.

5. Conclusions

In this paper a new soft switching buck and boost is introduced. The soft switching is achieved for full load range while the control circuit remains PWM. The converter is analyzed and its different operating modes are presented. Design considerations are discussed and a laboratory prototype is implemented. The presented experimental results confirm the validity of theoretical analysis.

References

[1] Hwang JC, Chen LH, Yeh SN. Comprehensive analysis and design of multi-leg fuel cell boost converter. J Appl Energy 2007:1274–88.
[2] Eakburanawat J, Boonyaroonate I. Development of a thermoelectric battery-charger with microcontroller-based maximum power point tracking technique. J Appl Energy 2006:687–704.
[3] Sabzali AJ, Ismail EH, Al-Saffar MA. Design criteria for modified zeta rectifier with reduced voltage stress and low effect on main. J Energy Convers Manage 2008:157–68.
[4] Dixon JW, Ortlizar ME. Ultracapacitors + DC–DC converters in regenerative braking system. IEEE AESS Syst Mag 2002:16–21.
[5] Rufer AE, Barrade PE, Hotellier D. Power–electronic interface for a supercapacitor-based energy-storage substation in DC-transportation networks. J EPE 2004;14:43–9.
[6] Adib E, Farzanehfard H. Family of zero current transition PWM converters. IEEE Trans Ind Electron 2008:3055–63.
[7] Adib E, Farzanehfard H. Family of isolated zero current transition PWM converters. J Power Electron 2009:156–63.
[8] Abdelhamid TH, Sabzali AJ. New three-phase ac–ac converter incorporating three-phase boost integrated ZVT bridge and single-phase HF link. J Energy Convers Manage 2008:1039–46.
[9] Yamamoto K, Hiraki E, Tanaka T, Nakaoka M, Mishima T. Bidirectional DC–DC converter with full-bridge/push–pull circuit for automobile electric power systems, presented at 37th IEEE PESC conference, Jeju, Korea, 18–22 June; 2006.
[10] Farzanehfard H, Beyragh DS, Adib E. A bidirectional soft switched ultracapacitor interface circuit for hybrid electric vehicle. J Energy Convers Manage 2008;49:3578–84.